Parametric Investigation of Laser-Induced Fluorescence of Solid-State Uranyl Compounds

Guangjun Wang, Yi Su, and David L. Monts*

Department of Physics and Astronomy, and Institute for Clean Energy Technology, Mississippi State University, Mississippi State, Mississippi 39762

Received: March 17, 2008; Revised Manuscript Received: July 31, 2008

The combination of remote/standoff sensing and laser-induced fluorescence (LIF) spectroscopy shows potential for detection of uranyl (UO_2^{2+}) compounds. Uranyl compounds exhibit characteristic emission in the 450−600 nm (22200 to 16700 cm^{-1}) spectral region when excited by wavelengths in the ultraviolet or in the short-wavelength portion of the visible spectrum. We report a parametric study of the effects of excitation wavelength [including 532 nm (18797 cm^{-1}), 355 nm (28169 cm^{-1}), and 266 nm (37594 cm^{-1})] and excitation laser power on solid-state uranium compounds. The uranium compounds investigated include uranyl nitrate, uranyl sulfate, uranyl oxalate, uranium dioxide, triuranium octaoxide, uranyl acetate, uranyl formate, zinc uranyl acetate, and uranyl phosphate. We observed the characteristic uranyl fluorescence spectrum from the uranium compounds except for uranium oxide compounds (which do not contain the uranyl moiety) and for uranyl formate, which has a low fluorescence quantum yield. Relative uranyl fluorescence intensity is greatest for 355 nm excitation, and the order of decreasing fluorescence intensity with excitation wavelength (relative intensity/laser output) is 355 nm > 266 nm > 532 nm. For 532 nm excitation, the emission spectrum is produced by two-photon excitation. Uranyl fluorescence intensity increases linearly with increasing laser power, but the rate of fluorescence intensity increase is different for different emission bands.

Introduction

Uranium in various forms has historically been present at a significant number of U.S. governmental facilities. The U.S. government has begun an extensive effort to address environmental problems relating to this nuclear legacy. Means of detection are required to locate contaminated areas for subsequent cleanup. Because of its very long half-lives (10^5-10^9 years depending upon the isotope), uranium is difficult to remotely detect in small quantities using radioactive counting techniques. Because uranium metal readily oxides, it is therefore useful to seek optically based means of screening for the presence of uranium oxide compounds.

It has long been known that uranyl (UO_2^{2+}) minerals yield an easily detectable, characteristic emission.[1−12] The absorption spectrum of uranyl compounds in the 345−500 nm (29000 to 20000 cm^{-1}) region is due to transitions to 12 excited electronic states.[13−15] Ultraviolet or shorter-wavelength visible excitation of uranyl compounds produces characteristic banded fluorescence emission in the 450−600 nm (22200 to 16700 cm^{-1}) spectral region. Typically four to six different vibronic emission bands are observed, regardless of the excitation wavelength. Radiationless processes rapidly transfer[13,16−18] the energy to the lowest excited state [$A^3\Delta g$ ($\Omega = 1_g$)] from which magnetic-dipole emission occurs to vibrational levels[5,8−10] in the ground electronic state [$X\ ^1\Sigma^+_g$ ($\Omega = 0^+_g$)] [13−15] of the uranyl moiety. The Laporte-forbidden uranyl emission has been commonly referred to as fluorescence in the literature. The overall intensity of the uranyl fluorescence is different for different uranyl compounds. There is also some variability of the emission wavelengths among different uranyl compounds.

In the early 1980s, Chimenti and co-workers[19,20] investigated the feasibility of quantitatively utilizing uranyl fluorescence to remotely sense uranyl ores. They successfully demonstrated the technical feasibility of LIF detection of uranyl minerals with a threshold limit of detection of 80 ppm, although some samples could be detected at tens of ppb. However, the expense of airborne exploration and questions about how the terrain might affect the signal lead to this option not being utilized for airborne remote sensing geologic exploration for uranium ores.

In the late 1990s, DiBenedetto and co-workers[21,22] developed a portable LIF system for standoff detection of uranyl compounds that are present as surface contaminants. The excitation wavelength was 532 nm, which is the second harmonic from a pulsed Nd:YAG laser. The system had an estimated threshold limit of 3000 dpm (which corresponds to about 4 mg of U-238) at a standoff distance of 8−10 feet (2.4−3.0 m). The design criteria required a cart-mounted portable system that could be pulled and operated by a single technician. The effort was terminated because there was insufficient battery life for operation of the compact, pulsed Nd:YAG laser without frequent battery changes.

Geipel and co-workers,[23−30] Moulin and co-workers,[31−39] and other groups[40−47] have utilized time-resolved laser-induced fluorescence spectroscopy (TRLIFS) in order to distinguish among the uranyl compounds. In TRLIFS, the fluorescence is recorded only during a selected temporal window, following a selected time delay. The advantage of TRLIFS over non-time-resolved LIF is the ability to distinguish one chemical species from a similar chemical species based upon the time profile of their fluorescent emission from a given medium. With regard to the challenge of remotely locating uranyl compounds in large facilities, we believe that uranyl species characterization will not be required and that species characterization might needlessly complicate the process since in general what is important is the presence of uranium, not which uranium compound is present. Consequently, the detection scheme that we are currently pursuing utilizes non-time-resolved LIF.

* To whom correspondence should be addressed. Telephone: (662) 325-2931. E-mail: DLM1@Ra.MsState.Edu.

10.1021/jp802327f CCC: $40.75
Published on Web 09/30/2008

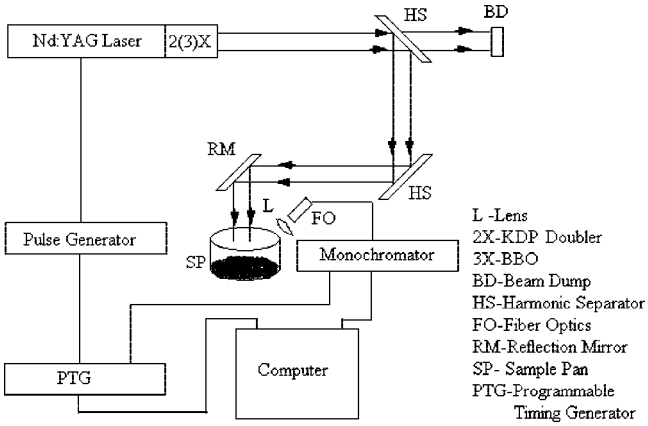

Figure 1. Schematic of LIF apparatus.

To develop an optical screening technique for the presence of solid-state uranyl compounds, we have investigated the dependence of uranyl LIF emission intensity on laser excitation wavelength and on laser power.

2. Experiment

Figure 1 presents a schematic of the experimental apparatus. The apparatus includes a laser, pulse generator, programmable timing generator, mirrors, monochromator, fiber optic pickup, sample pan, and data acquisition computer. We used a 10 Hz pulsed Nd:YAG laser (Quanta-Ray, DCR-4) for 532, 355, and 266 nm excitation wavelengths and a continuous wave (cw) diode laser (TOPTICA Photonics, DL-100) for 409 nm. Typical laser pulse energies were 20 mJ/pulse for 266, 355, and 532 nm excitation; at 409 nm, 3 mW cw excitation was employed. When the Nd:YAG laser was used, the desired excitation wavelength was separated from the other Nd:YAG wavelengths using dichroic mirrors (CVI Lasers). A pulse generator (Stanford Research Systems, DG535) triggered by the Nd:YAG laser Q-switch was used to correct the irregular form of the laser's Q-switch trigger and adjust the delay time for the programmable timing generator (PTG; Princeton Instruments, ST133A) that controls operation of the blue-sensitive, thermoelectrically cooled, data acquisition intensified charged-coupled device (ICCD) camera (Princeton Instruments, PI-MAX MG 1KSB). Synchronization of the laser pulse and the ICCD was optimized using a 200 MHz digital oscilloscope (Tektronix, TDS 420A). Typical gate widths were 500 μs for 266, 355, and 532 nm pulsed excitation and 25 ms for 409 nm cw excitation. The ICCD detector is mounted on a 0.5 m imaging triple-grating monochromator (Acton Research Corp., SpectraPro 500i) with a 1200-groove/mm diffraction grating (blazed at 500 nm). The fiber optic pickup (Oriel, 77644) was placed about 1−2 cm from the sample. Uranium compound solids were poured into aluminum weighing pans; sufficient sample was added to completely cover the bottom of the pan in order to avoid reflection of the laser beam. The excitation laser beam was directed downward toward the sample. The laser pulse energy dependence of the signal intensity was investigated by varying the flashlamp pulse energy of the Nd:YAG laser and measuring the Nd:YAG laser power with a laser power meter (Scientech).

The following solid-state uranium compounds (purity, 99.98%) were investigated: uranyl formate $UO_2(HCOO)_2 \cdot 3H_2O$ (Electron Microscopy Sciences); uranyl nitrate $UO_2(NO_3)_2 \cdot 6H_2O$ (Alfa Æsar); uranyl phosphate $UO_2HPO_4 \cdot 4H_2O$ (International Bio-Analytical Industries); uranyl sulfate $UO_2SO_4 \cdot 3H_2O$ (International Bio-Analytical Industries); uranium dioxide UO_2 (International Bio-Analytical Industries); and triuranium octaoxide U_3O_8 (International Bio-Analytical Industries). In addition, the following solid-state uranyl compounds obtained from the university's radiation safety officer were also studied: uranyl acetate $UO_2(C_2H_3O_2)_2 \cdot 2H_2O$ (Baker); uranyl oxalate $UO_2C_2O_4 \cdot 3H_2O$ (Polysciences); and zinc uranyl acetate $ZnUO_2(CH_3COO)_4 \cdot 2H_2O$ (Pfaltz & Bauer). All the chemicals were used without further purification and were chosen for their availability.

TABLE 1: Effect of Excitation Wavelength upon Presence or Absence of Laser-Induced Fluorescence from Nine Selected Solid-State Uranium Compounds ("Yes",Observation of LIF Spectrum; "No", No LIF Spectrum Observed)

compound	266 nm excitation	355 nm excitation	409 nm excitation	532 nm excitation
uranyl acetate	yes	yes	yes	yes
uranyl formate	no	no	no	no
uranyl nitrate	yes	yes	yes	yes
iranyl oxalate	yes	yes	yes (weak)	yes (weak)
uranyl phosphate	yes	yes	yes	yes
uranyl sulfate	yes	yes	yes	yes
zinc uranyl acetate	yes	yes	yes (weak)	yes (weak)
UO_2	no	no	no	no
U_3O_8	no	no	no	no

3. Results and Discusssion

It has been long known that some uranyl salts exhibit emission with distinctive spectral characteristics.[1−12] The literature reports that the emission wavelength and intensity are different for different uranyl compounds.[5,8,24,25,38,45−47] The wavelength variability of different uranyl compounds has been attributed to the effect of ligands and of the media.[8,11,12] To develop an optically based screening technique for uranium compounds, we have investigated the effect of excitation wavelength and of laser power on uranyl fluorescence.

We have studied the laser-induced emission spectra of a total of nine different solid-state uranium compounds, seven of which are uranyl salts and two are uranium oxides. Of the seven uranyl salts, we detected fluorescence from six (see Table 1). No emission was detected for uranyl formate or for the uranium oxides with any of the excitation wavelengths investigated.

We detected no emission from solid-state uranyl formate trihydrate at room temperature at any of the excitation wavelengths (266, 355, 409, and 532 nm) employed in this investigation. Our inability to detect uranyl formate fluorescence was replicated on different days with different samples; substitution of another uranyl compound for uranyl formate yielded fluorescence. Some uranyl compounds (such as uranyl carbonate) fluoresce at low temperature but not at room temperature.[30,40,46] The behavior of uranyl carbonate is attributed to the temperature-dependent quenching effect of carbonate.[48] There are also some uranyl minerals, such as torbernite $(Cu(UO_2)_2(PO_4)_2 \cdot 10H_2O)$,[19] metatorbernite $(Cu(UO_2)_2(PO_4)_2 \cdot 8H_2O)$,[19] and chernikovite $((H_3O)_2(UO_2)_2(PO_4)_2 \cdot 6H_2O)$,[25] that do not fluoresce either at room temperature or at cryogenic temperatures. Using mercury lamp excitation, the fluorescence spectra of uranyl formate monohydrate and of anhydrous uranyl formate have been observed by Claudel and Sautereau at 77 K and also at 298 K.[49] West et al.[50] have reported the fluorescence excitation spectrum of uranyl formate monohydrate at 4.2 K; they used a dye laser to scan the spectrum near 469 nm (21322 cm^{-1}) and monitored the emission intensity at 507.25 nm (19714 cm^{-1}). We believe that our inability to observe uranyl formate

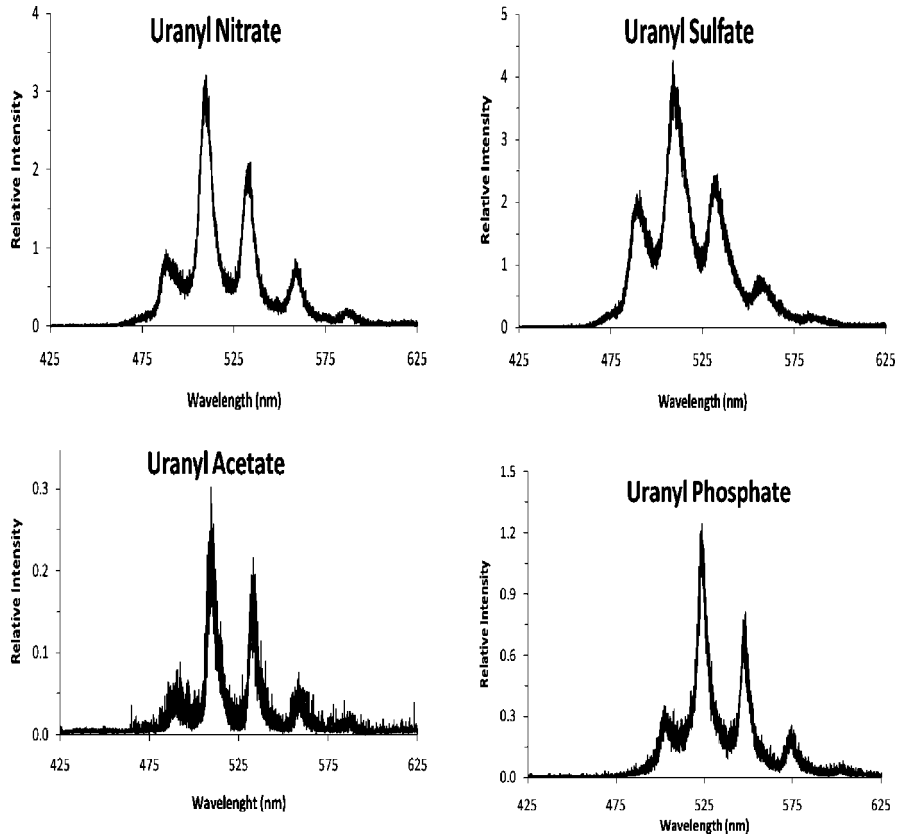

Figure 2. Laser-induced emission spectra of four selected solid-state uranyl compounds excited at 355 nm with 0.2 W average power. For all compounds shown, the emission spectra were obtained by adding two spectra.

fluorescence is related to its low fluorescence quantum efficiency Φ [4.5×10^{-4} for monohydrate[51] and 6.3×10^{-3} for anhydrous[51]], which is significantly lower than for other uranyl compounds.[7,8,12,16] The fluorescence quantum efficiency of some uranyl compounds approaches unity. Thus our inability to detect uranyl formate monohydrate fluorescence is related to the sensitivity of our detection system for the experimental conditions used.

Halverson and co-workers[52] have reported that UO_2, UO_3, and U_3O_8 fluoresce weakly when excited with 355 or 266 nm radiation; the fluorescence peak wavelength depends upon the excitation wavelength, but all fluoresce in the 500−540 nm region. We believe that the fluorescence quantum efficiencies of UO_2, UO_3, and U_3O_8 are probably significantly lower than those of most uranyl compounds.[7,8,12,16] Hence, our inability to detect uranium oxide fluorescence is related to the sensitivity of our detection system for the experimental conditions used. Therefore, we do not expect to observe any uranium oxide fluorescence unless the uranium oxide concentration is relatively large and is much larger than the uranyl concentration. Since our goal is a screening technique for detecting the presence of uranium compounds, uranium oxide fluorescence would not be a spectral interference for our purposes.

Figure 2presents the laser-induced emission spectra (for 355 nm excitation) of four selected solid-state uranyl compounds. The same experimental conditions (same laser power, same detection gate width, and addition of two spectra) were used for all the compounds shown in Figure 2. Typically four to six vibronic emission bands are observed. The uranyl vibronic emission is associated with transitions involving the O═U═O symmetric stretching vibration in the ground electronic state.[10] As these spectra show, the essential emission pattern is the same in all the cases, although there is significant variation in emission intensity, emission bandwidth, and, to a lesser extent, emission wavelength; this is consistent with results reported by others.[5,8,24,25,38,45−47] Of the four compounds shown in Figure 2, uranyl phosphate has the largest variation (∼14 nm) in emission wavelength. Typically the 509 nm (19646 cm^{-1}) emission band is the most intense and the 533 nm (18762 cm^{-1}) emission the next most intense, although the relative intensity of these two emissions varies among uranyl compounds and for zinc uranyl acetate, the two have comparable intensity. For uranyl phosphate, the 523.5 nm (19102 cm^{-1}) emission band is the most intense and the 548 nm (18248 cm^{-1}) emission band the next most intense. Comparison of the strongest emission band intensities indicates that the relative emission intensities of uranyl sulfate:uranyl nitrate:uranyl phosphate:uranyl acetate are about 14:11:4:1, respectively, for 355 nm excitation (Figure 2). Table 2 presents the emission wavelengths and bandwidth of the four most intense emission bands for four selected uranyl compounds. As Figure 2 and Table 2 illustrate there is significant variation in the bandwidth (fwhm, full width at half-maximum) of individual emission bands for different uranyl compounds. The variation in bandwidth occurs not only for different uranyl compounds (varying from an average fwhm of 6.5 nm for uranyl phosphate and of 17 nm for uranyl sulfate), but also for different emission bands of a given compound (the average fwhm of the two stronger emission bands tend to be smaller than those of the two weaker emission bands). The fwhms are comparable to those previously reported for uranyl compounds at room temperature.[8,9,25,38]

The effect of excitation wavelength upon the LIF emission of uranyl nitrate is presented in Figure 3. For all excitation wavelengths (266, 355, 409, and 532 nm), the entire emission spectrum is observed. Table 3 compares the emission wavelengths and bandwidths as a function of excitation wavelength for uranyl nitrate. For different excitation wavelengths, the band

TABLE 2: Comparison of Emission Wavelengths and Bandwidths of the Four Most Intense Emission Bands with 355 nm Excitation for Four Selected Solid-State Uranyl Compounds[a]

	uranyl nitrate	uranyl sulfate	uranyl acetate	uranyl phosphate	average bandwidth
	488	491.5	489	502	
	(13)	(14)	(11)	(6)	(11)
	509	510.5	509	523.5	
	(8)	(16)	(5)	(6)	(9)
	533	532.5	533	548	
	(8)	(17)	(6)	(7)	(9.5)
	560	558	558	574	
	(10)	(22)	(9)	(7)	(12)
average bandwidth	(10)	(17)	(8)	(6.5)	

[a] The top number is the emission band center (nm), and the lower number in parentheses is the fwhm bandwidth (nm). The right-most column contains the average bandwidths (FWHM) of its associated row; the bottom row contains the average bandwidths (FWHM) of the associated column.

centers are the same and fwhm bandwidths are almost the same for a given uranyl compound. For our application, detection will be accomplished by spectral imaging of a laser-irradiated area; the most convenient means of implementing this is to use narrow bandpass ("notch") filter(s) in conjunction with a spectral imaging camera. It is convenient to use one set of notch filters for detection of all fluorescing uranyl compounds and for all excitation wavelengths. For optical bandpass filters, there is a tradeoff between the width of the spectral range passed and the transmission efficiency: in general, the narrower the bandpass, the lower the transmission efficiency, and hence the higher the minimum detectable limit. To optimize uranyl LIF detection efficiency for our screening technique, we plan to utilize a notch filter that transmits both the 509 and 533 nm emission bands.

For 532 nm (18797 cm^{-1}) excitation, the excitation energy is less than 20502 cm^{-1} (487.8 nm), which is the uranyl (0,0) transition energy to the lowest excited electronic state.[10] Consequently observation of uranyl emission bands for 532 nm excitation (Figure 3, Table 3) indicates that two-photon absorption occurs. For uranyl oxalate and zinc uranyl acetate, fluorescence was observed with 532 nm excitation, but it was too weak to record. The occurrence of two-photon uranyl absorption has previously been reported. Zhdanov observed photoluminescence resulting from two-photon excitation using a ruby laser (694.3 nm, 14403 cm^{-1}). [53] Denning and co-workers have recorded two-photon laser excitation spectra of two uranyl compounds using tunable dye lasers.[13,54,55] Since the radiative lifetime of the lowest excited state of uranyl $*UO_2^{2+}$ is long (hundreds of microseconds),[9,16,56] electric dipole-allowed absorption from $*UO_2^{2+}$ to higher excited states has been reported by several researchers.[56−59] Observation of the typical uranyl emission bands for 532 nm excitation likely results from a two-photon absorption to a higher excited electronic state, which rapidly[13,16−18] relaxes to $*UO_2^{2+}$ from which all the usual emission transitions are observed.

It should be noted that the relative intensity of the 355 nm emission spectrum is greater than that of the 266 nm emission spectrum, which in turn is greater than that of the 532 nm excitation spectrum (Figure 3). All the emission spectra presented in Figure 3 were recorded using the same experimental conditions (addition of two spectra, same laser power, and same detection gate width). In the case of the 509 nm emission band of uranyl nitrate (Figure 3), the apparent ratio of emission intensity for 266:355:532 excitation is approximately 3:20:1. Consequently, the emission intensity of the 355 nm emission spectrum is significantly greater than that of the other excitation wavelengths. This wavelength-dependent intensity pattern is also true for the other solid-state uranyl compounds investigated. Since the origin of the lowest excited electronic state (20502 cm^{-1}, 487.8 nm)[10] is at higher energy than 532 nm (18797 cm^{-1}), the low emission intensity for 532 nm excitation is expected. Uranyl absorption coefficients in the deep ultraviolet have been reported by McGlynn and Smith[7] and by Bell and Biggers.[10] For an aqueous solution of uranyl nitrate, the uranyl molar extinction coefficient at 266 nm is about 40 times larger than at 355 nm,[7] while for an aqueous solution of uranyl perchlorate, the uranyl molar absorptivity coefficient at 266 nm is about 120 times larger than at 355 nm.[10] Previous laser spectroscopy investigations of uranyl fluorescence have employed a variety of ultraviolet excitation wavelengths, including 355 nm excitation[35,38,45,58] and 266 nm excitation.[24,25,38,40,45] To our knowledge, the only comparison of uranyl fluorescence intensity with 355 nm excitation and with 266 nm excitation is that reported by Moulin and co-workers.[38] They reported that in solution, the UO_2^{+2} fluorescence intensity is 10 times smaller with 355 nm excitation than with 266 nm excitation. These reported solution phase results lead to the expectation that the uranyl fluorescence intensity should be greater with 266 nm excitation rather than with 355 nm excitation, which is the opposite of what we observed with solid-state samples. The reason for this difference is not understood. It should be noted in passing that Halverson and co-workers observed higher fluorescence intensity with 355 nm excitation than with 266 nm excitation for solid UO_2, solid UO_3, and aqueous U_3O_8.[52]

To investigate the feasibility of utilizing a 409 nm cw diode laser rather than a pulsed Nd:YAG laser for excitation, excitation spectra were also recorded using a diode laser. We observed fluorescence from the same uranium compounds with cw 409 nm excitation that we observed with Nd:YAG excitation (Table 1). Using a longer data acquisition time (25 ms for cw excitation vs 500 μs for pulsed excitation), emission spectra of quality comparable to those recorded with 355 nm excitation were obtained. Since the experimental conditions are different, a direct quantitative comparison of the relative emission intensities obtained with 409 nm cw excitation and pulsed excitation is not possible, but the use of a cw diode laser is a viable alternative to pulsed Nd:YAG excitation. Comparing the Nd:YAG laser with the diode laser, we find that diode laser has three advantages over use of a Nd:YAG laser. One is the diode laser's size and weight, since it is much smaller and lighter. Another is that the diode laser can operate using low-current, 115-VAC electrical power. The last one is that the diode laser is a continuous source and hence has a much higher duty cycle. The Nd:YAG laser's advantage is its much higher laser pulse energy. For designing a portable detection system for uranyl compounds, a short wavelength diode laser offers many advantages.

The dependence of the uranyl emission upon pulsed laser excitation power was examined. The results are shown in Figure 4 for uranyl nitrate and uranyl sulfate for 532, 355, and 266 nm excitation. For each of the excitation wavelengths, the laser power dependence is seen to be linear as verified by a linear regression fit of the natural logarithm of the relative fluorescence intensity as a function of the natural logarithm of the laser power. For the highest laser excitation powers used, the emission intensity is beginning to deviate from linearity. At the higher laser powers, the duration of the measurement had to be limited to obtain reliable results. If the sample was exposed to the laser

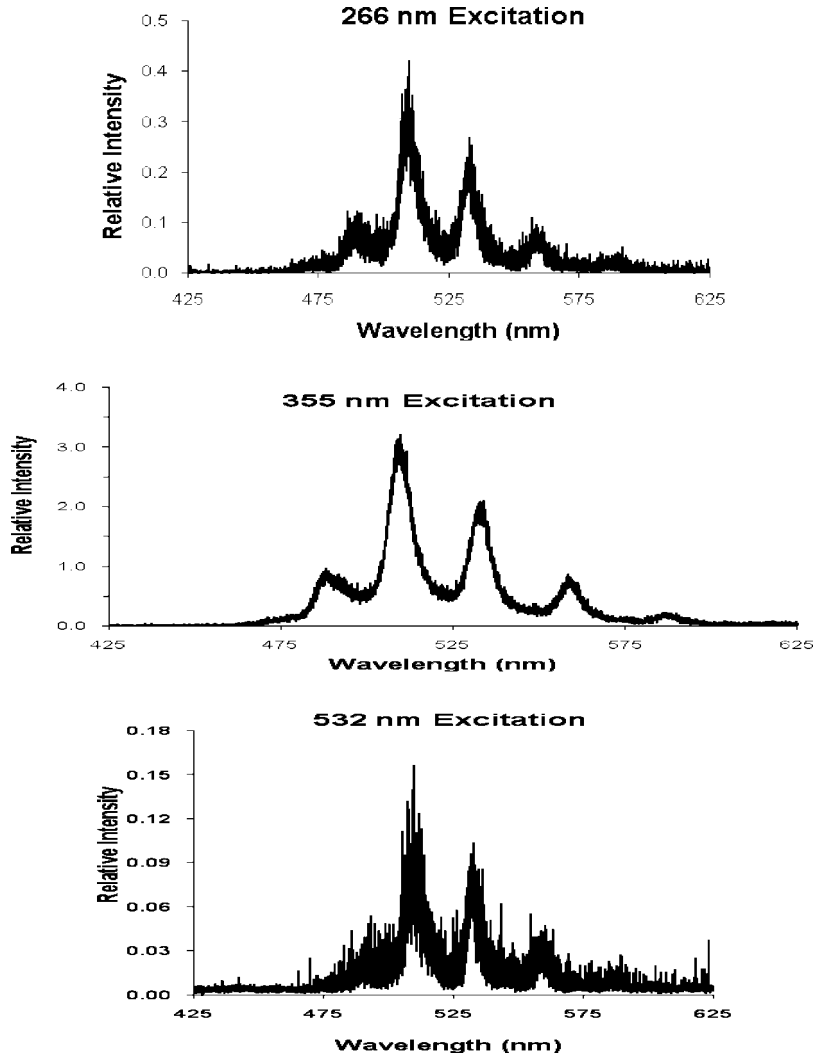

Figure 3. Laser-induced emission spectra of solid-state uranyl nitrate as a function of excitation wavelength. The emission spectra were obtained by adding two spectra together. The laser excitation powers were 0.2 W for all excitation wavelengths.

TABLE 3: Comparison of Emission Wavelengths and Bandwidths of the Four Most Intense Emission Bands As a Function of Excitation Wavelength for Solid-State Uranyl Nitrate[a]

(υ',υ'')	266 nm	355 nm	532 nm
(0,0)	488	488	488
	(14)	(13)	(14)
(0,1)	509	509	509
	(8)	(8)	(9)
(0,2)	533	533	533
	(8)	(8)	(9)
(0,3)	560	560	560
	(10)	(10)	(11)

[a] The top number is the emission band center (nm), and the lower number in parentheses is the fwhm bandwidth (nm). The vibrational quantum number of the uranyl symmetric stretching vibration in the upper electronic state is designated by υ' and in the lower electronic state by υ''.[10]

beam for extended periods of time, the yellow uranyl compounds were observed to turn gray or black where the Nd:YAG laser beam (approximately 1 cm diameter) irradiated the sample. The cause of the color change is probably due to photochemical reduction of U(VI) to U(V) and U(IV)[8,12,60−66] or in the language of solid state physics, to the formation of color centers.[12,67−69] The data in Figure 4 were fit using linear regression in Microsoft EXCEL spreadsheets; the slopes of the resulting linear fits are presented in Table 4. As Figure 4 shows and Table 4 documents, the rate of emission intensity increase is different for different uranyl emission bands, specifically the rate of emission intensity increases with increasing laser power and decreases in the order 509 nm > 533 nm > 488 nm ∼560 nm > 587 nm. This ordering is also the ordering for the relative emission intensities among the uranyl vibronic emission bands. Hence, the different rates of emission intensity increase may be related to the transition probabilities.

4. Conclusions

The distinctive spectral emission features of uranyl compounds enable remote detection. Use of LIF technology enables a convenient means of surveying areas suspected of contamination by uranyl compounds. From our study of the LIF emission spectra of these solid-state uranyl compounds, we find that the uranyl emission intensity exhibits a significant dependence on the excitation wavelength and laser intensity. The emission spectra of these solid-state samples display similar spectral features, but the relative emission intensity is a function of excitation wavelength with the fluorescence intensity for 355 nm excitation being significantly greater than that for 266 nm, which in turn is greater than 532 nm excitation. Fluorescence emission from uranyl oxalate or zinc uranyl acetate was detected

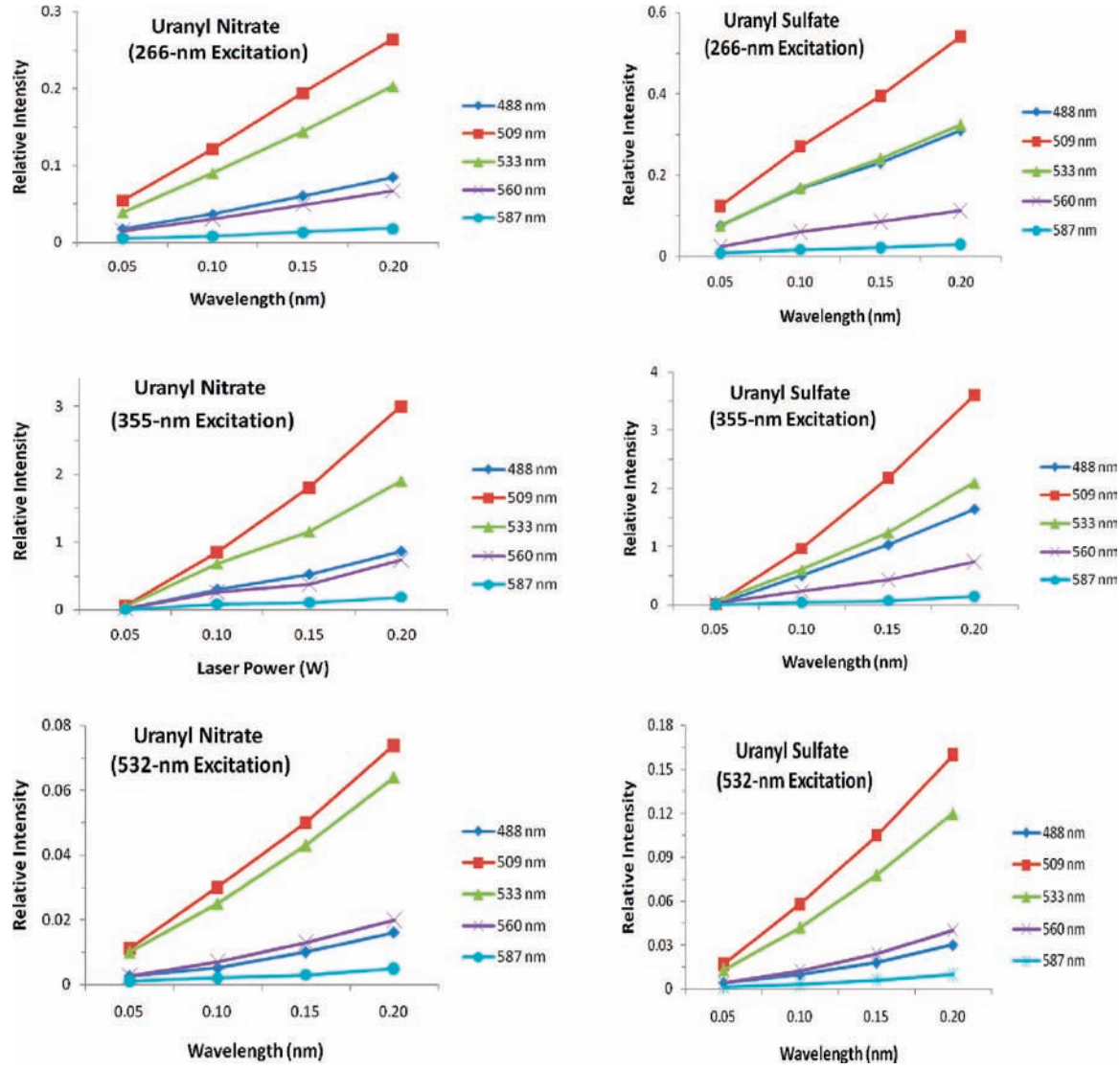

Figure 4. Laser power dependence of solid-state uranyl nitrate and of solid-state uranyl sulfate as a function of excitation wavelength and of emission band monitored. The emission spectra were obtained by adding two spectra together.

TABLE 4: Slope of Laser Power Dependence for Relative Intensity of Different Emission Bands of Solid-State Uranyl Nitrate and Uranyl Sulfate as a Function of Excitation Wavelength[a]

emission band (nm)	532 nm	355 nm	266 nm
	Uranyl Sulfate		
488 (0,0)	0.17	10.9	1.5
509 (0,1)	0.95	24.0	2.7
533 (0,2)	0.71	13.6	1.6
560 (0,3)	0.24	4.7	0.59
587 (0,4)	0.06	0.90	0.14
	Uranyl Nitrate		
488 (0,0)	0.09	5.5	0.45
509 (0,1)	0.42	19.6	1.4
533 (0,2)	0.36	12.1	1.1
560 (0,3)	0.12	4.6	0.35
587 (0,4)	0.03	1.1	0.09

[a] Emission bands are identified by peak wavelength (nm) and by (v',v'') designation of vibrational levels involved.[10]

with 532 nm excitation, but was too weak to be recorded; and no emission was detected with any of the excitation wavelengths investigated for UO_2 or U_3O_8. Thus, a laser-induced fluorescence-based screening technique is limited to uranyl compounds and will not efficiently detect uranium oxides. The uranyl emission intensity increases linearly with increasing laser power (for the laser powers investigated), but increases at different rates for different uranyl emission bands. Hence, there are two ways to increase sensitivity: one is to increase the laser power and the other is to use appropriate wavelength excitation. Given the limit of available laser powers, the more realizable approach is to use a laser of short wavelength, but close to the absorption maximum.

Acknowledgment. This work was supported by funding from the U.S. Department of Energy through Cooperative Agreement DE-FC01-06EW-07040 and subsequently by funding from the U. S. Department of Defense/U. S. Army Engineer Research and Development Center grant W912HZ-06-C-0032. We thank Mr. Michel E. Okhuysen (Mississippi State University) for his assistance with the initial setup of the detection equipment. We also thank the reviewer for making us aware of the fluorescence behavior of uranyl carbonate.

References and Notes

(1) Brewster, D. *Trans. R. Soc. Edinburgh* **1833**, 12.
(2) Stokes, G. G. *Philos. Trans. R. Soc. London* **1852**, *142*, 517.

(3) Becquerel, E. C.R. *Acad. Sci.* **1872**, *75*, 296.
(4) Nichols, E. L.; Howes, H. L. *Fluorescence of the Uranyl Salts*; Carnegie Institute of Washington: Washington, DC, 1919.
(5) Dieke, G. H.; Duncan, A. B. F. *Spectroscopic Properties of Uranium Compounds*; National Nuclear Energy Series, Division III, Vol. 2; McGraw-Hill: New York, 1949.
(6) Haberlandt, H.; Hernegger, F.; Scheminzky, F. *Spectrochim. Acta* **1950**, *4*, 21.
(7) McGlynn, S. P.; Smith, J. K. *J. Mol. Spectrosc.* **1961**, *6*, 164.
(8) Rabinowitch, E; Belford, R. L. *Spectroscopy and Photochemistry of Uranyl Compounds*; Pergamon: New York, 1964/.
(9) Bell, J. T.; Biggers, R. E. *J. Mol. Spectrosc.* **1965**, *18*, 247.
(10) Bell, J. T.; Biggers, R. E. *J. Mol. Spectrosc.* **1968**, *25*, 312.
(11) Görller-Walrand, C.; de Jaegere, S *Spectrochim. Acta A* **1972**, *28*, 257.
(12) Burrows, H. D.; Kemp, T. J. *Chem. Soc. Rev.* **1974**, *3*, 139.
(13) Denning, R. G. *Struct. Bonding (Berlin)* **1992**, *79*, 215.
(14) Matsika, S.; Pitzer, R. M. *J. Phys. Chem. A* **2001**, *105*, 637.
(15) Matsika, S.; Zhang, Z.; Brozell, S. R.; Blaudeau, J.-P.; Wang, Q.; Pitzer, R. M. *J. Phys. Chem. A* **2001**, *105*, 3825.
(16) Sugitani, Y.; Nomura, H.; Nagashima, K. *Bull. Chem. Soc. Jpn.* **1980**, *53*, 2677.
(17) Thorne, J. R. G.; Denning, R. G.; Barker, T. J.; Grimley, D. I. *J. Lumin.* **1985**, *34*, 147.
(18) Azenha, M. E. D. G.; Burrows, H. D.; Formosinho, S. J.; Miguel, M. G. M.; Daramanyan, A. P.; Khudyakov, I. V. *J. Lumin.* **1991**, *48*, 522.
(19) deNeufville, J. P.; Kasdan, A.; Chimenti, R. J. L. *Appl. Opt.* **1981**, *20*, 1279.
(20) Kasdan, A.; Chimenti, R. J. L.; deNeufville, J. P. *Appl. Opt.* **1981**, *20*, 1297.
(21) DiBenedtto, J.; Abbott, R.; Capelle, G.; Chavez, G.; Lutz, S.; Tesar, J. Airborne and Ground Based Laser Induced Fluorescence Imaging (LIFI). In *Optical Remote Sensing for Environmental and Process Monitoring*, SPIE Vol. 2883; Romano, R. R., Ed.; SPIE: Bellingham, WA, 1996; pp 255−266.
(22) U.S. Department of Energy, Airborne laser induced fluorescence imaging, DOE/EM-0427, Office of Environmental Management, Office of Science and Technology, 1999; http://apps.em.doe.gov/ost/pubs/itsrs/itsr78.pdf.
(23) Geipel, G.; Brachmann, A.; Brendler, V.; Bernhard, G.; Nitsche, H. *Radiochim. Acta* **1996**, *75*, 199.
(24) Rutsch, M.; Geipel, G.; Brendler, V.; Bernhard, G.; Nitsche, H. *Radiochim. Acta* **1999**, *86*, 135.
(25) Geipel, G.; Bernhard, G.; Rutsch, M.; Brendler, V.; Nitsche, H. *Radiochim. Acta* **2000**, *88*, 757.
(26) Gabriel, U.; Charlet, L.; Shläpfer, C. W.; Vial, J. C.; Brachmann, A.; Geipel, G. *J. Colloid Interface Sci.* **2001**, *239*, 358.
(27) Amayri, S.; Arnold, T.; Foerstendorf, H.; Geipel, G.; Bernhard, G. *Can. Mineral.* **2004**, *42*, 953.
(28) Amayri, S.; Arnold, T.; Reich, T.; Foerstendorf, H.; Geipel, G.; Bernhard, G.; Massanek, A. *Environ. Sci. Technol.* **2004**, *38*, 6032.
(29) Baumann, N.; Arnold, T.; Geipel, G.; Truman, E. R.; Black, S.; Read, D. *Sci. Total Environ.* **2006**, *366*, 905.
(30) Geipel, G. *Coord. Chem. Rev.* **2006**, *250*, 844.
(31) Deniau, H.; Decambox, P.; Mauchien, P.; Moulin, C. *Radiochim. Acta* **1993**, *61*, 23.
(32) Moulin, C.; Rougeault, S.; Hamon, D.; Mauchien, P. *Appl. Spectrosc.* **1993**, *47*, 2007.
(33) Couston, L.; Pouyat, D.; Moulin, C.; Decambox, P. *Appl. Spectrosc.* **1995**, *49*, 349.
(34) Moulin, C.; Decambox, P.; Moulin, V.; Decaillon, J. G. *Anal. Chem.* **1995**, *67*, 348.
(35) Moulin, C.; Decambox, P.; Mauchien, P.; Pouyat, D.; Couston, L. *Anal. Chem.* **1996**, *68*, 3204.
(36) Moulin, C; Decambox, P.; Mauchien, P. *J. Radioanal. Nucl. Chem.* **1997**, *226*, 135.
(37) Scapolan, S.; Ansoborlo, E.; Moulin, C.; Madic, C. *J. Radioanal. Nucl. Chem.* **1997**, *226*, 145.
(38) Moulin, C.; Laszak, I.; Moulin, V.; Tondre, C. *Appl. Spectrosc.* **1998**, *52*, 528.
(39) Moulin, C.; Charron, N.; Plancque, G.; Virelizier, H. *Appl. Spectrosc.* **2000**, *54*, 843.
(40) Kato, Y.; Meinrath, G.; Kimura, T.; Yoshida, Z. *Radiochim. Acta* **1994**, *64*, 107.
(41) Eliet, V.; Bidoglio, G.; Omenetto, N.; Parma, L.; Grenthe, I. *J. Chem. Soc., Faraday Trans.* **1995**, *91*, 2275.
(42) Meinrath, G. *J. Radioanal. Nucl. Chem.* **1997**, *224*, 119.
(43) Eliet, V.; Grenthe, I.; Bidoglio, G. *Appl. Spectrosc.* **2000**, *54*, 99.
(44) Addleman, R. S.; Wai, C. M. *Anal. Chem.* **2000**, *72*, 2109.
(45) Billard, I.; Ansoborlo, E.; Apperson, K.; Arpigny, S.; Azenha, M. E.; Birch, D.; Bros, P.; Burrows, H. D.; Choppin, G.; Couston, L.; DuBois, V.; Fanghänel, T.; Geipel, G.; Hubert, S.; Kim, J. I.; Kimura, T.; Klenze, R.; Kronenberg, A.; Kumke, M.; LaGarde, G.; LaMarque, G.; Lis, S.; Madic, C.; Meinrath, G.; Moulin, C.; Nagaishi, R.; Parker, D.; Plancque, G.; Scherbaum, F.; Simoni, E.; Sinkov, S.; Viallesoubranne, C. *Appl. Spectrosc.* **2003**, *57*, 1027.
(46) Wang, Z.; Zachara, J. M.; Yantasee, W.; Gassman, P. L.; Liu, C.; Joly, A. G. *Environ. Sci. Technol.* **2004**, *38*, 5591.
(47) Wang, Z.; Zachara, J. M.; Gassman, P. L.; Liu, C. X.; Qafoku, O.; Yantasee, W.; Catalano, J. G. *Geochim. Cosmochim. Acta* **2005**, *69*, 1391.
(48) Balzani, V.; Bolletta, F.; Gandolfi, M. T.; Maestri, M. *Top. Curr. Chem.* **1978**, *75*, 1.
(49) Claudel, B.; Sautereau, H. *Spectrochim. Acta A* **1973**, *29*, 1687.
(50) West, W. P.; Muller, C. H., III; Porter, J. T., II; Malley, M. M. *J. Chem. Phys.* **1983**, *78*, 3338.
(51) Claudel, B.; Feve, M.; Puaux, J. P.; Sautereau, H. *J. Photochem.* **1977**, *7*, 113.
(52) Halverson, J.; Pan, Y. L.; Chang, R. K. Distinguishing micron-sized UO_2, UO_3, etc., particles from other common mineral particles by single-shot fluorescence spectra, WSRC-MS-2002-00948, 2003; http://www.osti.gov/energycitations/product.biblio.jsp?osti_id=807673.
(53) Zhdanov, A. A. *Sov. Phys. Dokl.* **1969**, *14*, 444.
(54) Barker, T. J.; Denning, R. G.; Thorne, J. R. G. *Inorg. Chem.* **1987**, *26*, 1721.
(55) Barker, T. J.; Denning, R. G.; Thorne, J. R. G. *Inorg. Chem.* **1992**, *31*, 1344.
(56) Jørgensen, C. K.; Reisfeld, R. *Struct. Bonding (Berlin)* **1982**, *50*, 121.
(57) Hill, R. J.; Kemp, T. J.; Allen, D. M.; Cox, A. *J. Chem. Soc., Faraday Trans. 1,* **1974**, *70*, 847.
(58) Sergeeva, G. I.; Chibisov, A. K.; Levshin, L. V.; Karyakin, A. V. *J. Photochem.* **1976**, *5*, 253.
(59) Bakac, A.; Burrows, H. D. *Appl. Spectrosc.* **1997**, *51*, 1916.
(60) Heidt, L. J.; Moon, K. A. *J. Am. Chem. Soc.* **1953**, *75*, 5803.
(61) Volman, D. H.; Seed, J. R. *J. Am. Chem. Soc.* **1964**, *86*, 5095.
(62) Mandelis, A. *Chem. Phys. Lett.* **1982**, *91*, 501.
(63) Wheeler, J.; Thomas, J. K. *J. Phys. Chem.* **1984**, *88*, 750.
(64) Monjushiro, H.; Hara, H.; Yokoyama, Y. *Anal. Sci., Suppl.* **1991**, *7*, 449.
(65) Dai, S.; Metcalf, D. H.; Del Cul, G. D.; Toth, L. M. *Inorg. Chem.* **1996**, *35*, 7786.
(66) Yusov, A. B.; Shilov, V. P. *Russ. Chem. Bull., Int. Ed.* **2000**, *49*, 1925.
(67) Tolstoi, N. A.; Abramov, A. P.; Abramova, I. N. *Opt. Spectrosc.* **1966**, *20*, 415.
(68) Tolstoi, N. A.; Abramova, I. N.; Abramov, A. P. *Opt. Spectrosc.* **1969**, *26*, 314.
(69) Bonch-Bruevich, A. M.; Kaliteevskaya, E. N.; Karapetyan, G. O.; Kolobkov, V. P.; Kudryashov, P. I.; Razumova, T. K.; Reishakhrit, A. L. *Opt. Spectrosc.* **1969**, *27*, 433.

JP802327F